Effect of diffusion and vessel topology on relaxation mechanisms using a cylinder fork model

Mohammed Salman Shazeeb[1] and Bashar Issa[1]
[1]*Department of Physics, UAE University, Al-Ain, Abu Dhabi, United Arab Emirates*

Introduction: Abstract#4727 has been submitted which proposes a cylinder fork model (CFM) to reflect the cortical vasculature in the brain and investigates the effect of vessel topology on R2 and R2* relaxation rates at different vessel diameters using simulations. The diffusion of protons due to random Brownian motion through magnetic field inhomogeneities is another factor that contributes to phase coherence changes and affects the relaxation rates [1]. Thus, the relaxation rates will depend upon the diffusion coefficient of spins that are within the vicinity of the induced field inhomogeneities due to the presence of vessels. The extent of effect will also depend upon the correlation time compared to the Larmor frequency variation at the surface of the vessel perturber [2], i.e., whether the diffusion rate falls in the fast (FXR), intermediate (IXR), or slow exchange regime (SXR). Since the state of water exchange differs between normal and tumor tissue [3], studying the effect of diffusion on relaxation times using the CFM could be interesting since the CFM incorporates a tortuous structure seen in tumors [4] as opposed to using straight 2D or 3D cylinders. In this study, we investigate the effect of diffusion rate on R2 and R2* relationship with the bifurcation angle of the CFM.

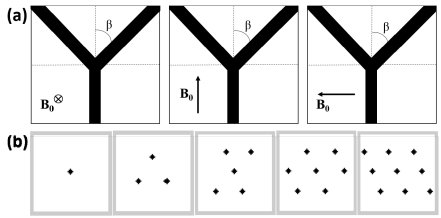

Fig. 1 – (a) Orientation of the cylinder fork (shown at 0<β<90) with respect to the magnetic field $\mathbf{B_0}$ shown in three different directions: into the page (orientation 1), up (orientation 2), and to the left (orientation 3) of the Y-shape cross-section. (b) Arrangement of straight cylinders (β=0) shown in 128×128 cross-sections.

Methods: Monte Carlo methods were used to quantify R2 and R2* for cylindrical fork perturbers at different bifurcation β angles with the magnetic field $\mathbf{B_0}$ oriented in three different directions (Fig. 1a). Details of all numerical values used in these simulations can be obtained from Abstract#4727. We modeled the vasculature using a CFM composed of straight trunk (prior to bifurcation) of half cube length and the bifurcating segments. The cube incorporates cylinder fork segments (Fig. 1b shows 1, 3, 5, 7 and 9 segments at β=0°) with varying β angles that were arranged close to symmetry without any overlapping vessels positioned in a parallel orientation. This model was converted into a 3D matrix and magnetic field perturbations were calculated using a forward 3D Fourier transform of the susceptibility distribution of the CFM [5]. The simulation was performed at true vessel diameters of 5 μm at three diffusion constant (D) values of 1×10^{-9}, 1×10^{-10} and 1×10^{-11} m^2/s. R2 and R2* were calculated by linear least-square fitting of log signal intensity versus volume fraction. Relaxation rates per volume fraction unit were used to remove the dependence on vessels length and emphasize the role of the β at different D values. Analysis of variance (ANOVA) test was used to check for any significant effects of D and β on the relaxation times. Percentage plots were used to accentuate differences of R2 and R2* per volume fraction unit at different β angles relative to the straight vessel across the different D values.

Results and Discussion: For all orientations, R2 and R2* show a clear dependence on the bifurcation angle β but with different behavior depending on the orientation (see Abstract#4727 for details). With a variation in D,

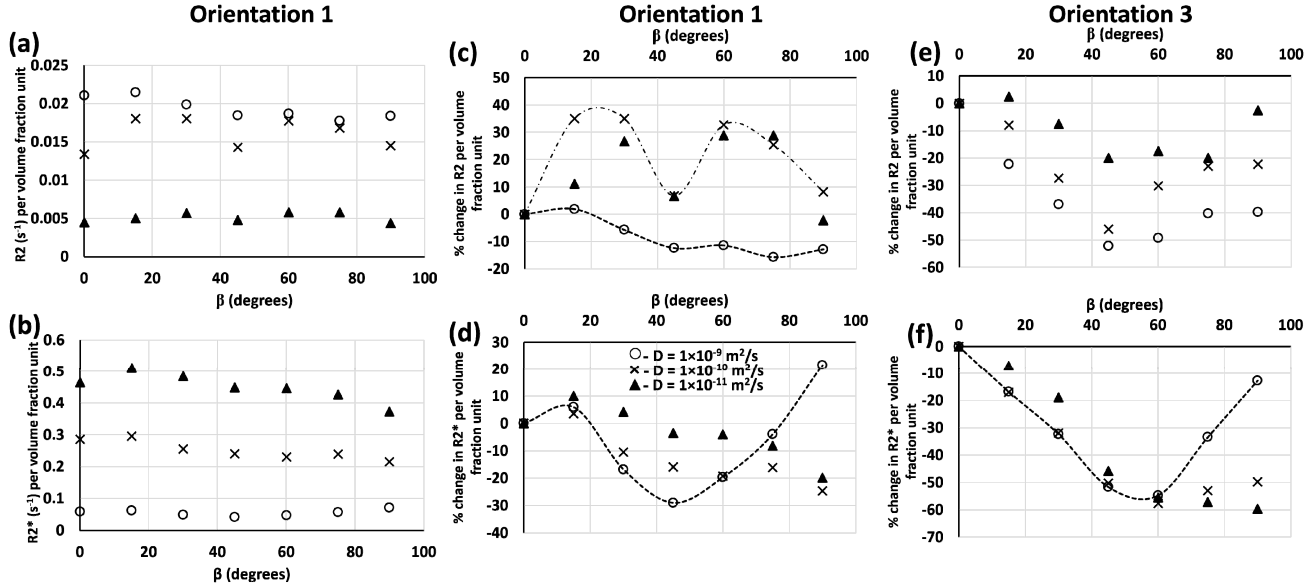

Fig. 2 – (a,b) Plots showing dependence of R2 and R2* per volume fraction unit with respect to β in orientation 1 at three different D values; (c,d) Plots showing percent change in R2 and R2* per volume fraction unit with respect to β in orientation 1 at three different D values; (e,f) Similar plots shown as (c,d) in orientation 3.

R2 and R2* showed differences with respect to β, particularly in orientations 1 and 3. R2 increased with D (Fig. 2a) while R2* decreased with D (Fig. 2b), which is indicative of a shift from the SXR towards the IXR/FXR [2]. At the highest D, R2 and R2* values are approaching each other at the respective β values indicating minimum loss of phase coherence, therefore heading towards the FXR. ANOVA test showed a significant effect of D ($p<0.002$) on R2 and R2* in all orientations. β only showed significant effects on R2 and R2* in orientations 2 and 3 ($p<0.03$). However, in orientation 1, an M-shape profile of R2 with respect to β is evident at the lower D values, which becomes less pronounced at the highest D value due to motion averaging (Fig. 2c). This effect is not so obvious in orientation 3 (Fig. 2e). With R2*, both orientations 1 and 3 show a distinctive V-profile with respect to β at the highest D value (Fig. 2d & 2f) while the lower D values show a decaying profile with β. These results clearly indicate a difference in R2 and R2* between the FXR and SXR with respect to β in some of the orientations. Since the apparent diffusion coefficient (ADC) is known to be lower, which corresponds to lower D values, in low-grade tumors [3], this CFM could potentially be used as a tool to differentiate normal vessels from tumor vessels based on a combination of β and D values.

Conclusion: Conventional methods use complicated models with multiple straight cylinders in a voxel to show relaxation time changes. Here, we demonstrate changes using a simple CFM that reflects the curvature of tumor vessels. R2 and R2* measurements indicate a clear dependence on β which varies between low and high D values. This model can further be developed to investigate relaxation effects of not just the bifurcation of vessels, but also in combination with diffusion parameters.

References: [1] Weisskoff *et al.* (1994). Magn Reson Med **31:**601-610; [2] Kennan *et al.* (1994). Magn Reson Med **31:**9-21; [3] Le Bihan *et al.* (1986). Radiol **161 :**401-407. [4] Coomber *et al.* (1988). J Neuropath Exp Neur **47:**29-40. [5] Marques and Bowtell (2005). Concept Magn Reson B **25B:**65-78.

Acknowledgments: This work was funded by UAE-NRF Grant 31S087.